

# The spatial clustering of ultraluminous infrared galaxies over $1.5 < z < 3$

D. Farrah

*Department of Astronomy, Cornell University, Ithaca, NY 14853, USA*

C. J. Lonsdale

*Infrared Processing Analysis Center, California Institute of Technology, Pasadena, CA  
91125, USA*

C. Borys

*Department of Astronomy and Astrophysics, University of Toronto, Toronto, Canada*

F. Fang

*Infrared Processing Analysis Center, California Institute of Technology, Pasadena, CA  
91125, USA*

I. Waddington & S. Oliver

*Astronomy Center, University of Sussex, Falmer, Brighton, UK*

M. Rowan-Robinson & T. Babbedge

*Astrophysics Group, Imperial College, London SW7 2BW, UK*

D. Shupe

*Infrared Processing Analysis Center, California Institute of Technology, Pasadena, CA  
91125, USA*

M. Polletta & H. E. Smith

*Center for Astrophysics and Space Sciences, University of California at San Diego, La  
Jolla, CA 92093, USA*

J. Surace

*Infrared Processing Analysis Center, California Institute of Technology, Pasadena, CA  
91125, USA*

## ABSTRACT

We present measurements of the spatial clustering of galaxies with stellar masses  $\gtrsim 10^{11} M_{\odot}$ , infrared luminosities  $\gtrsim 10^{12} L_{\odot}$ , and star formation rates  $\gtrsim 200 M_{\odot} \text{yr}^{-1}$  in two redshift intervals;  $1.5 < z < 2.0$  and  $2 < z < 3$ . Both samples cluster very strongly, with spatial correlation lengths of  $r_0 = 14.40 \pm 1.99 h^{-1} \text{Mpc}$  for the  $2 < z < 3$  sample, and  $r_0 = 9.40 \pm 2.24 h^{-1} \text{Mpc}$  for the  $1.5 < z < 2.0$  sample. These clustering amplitudes are consistent with both populations residing in dark matter haloes with masses of  $\sim 6 \times 10^{13} M_{\odot}$ , making them among the most biased galaxies at these epochs. We infer, from this and previous results, that a minimum dark matter halo mass is an important factor for all forms of luminous, obscured activity in galaxies at  $z > 1$ , both starbursts and AGN. Adopting plausible models for the growth of DM haloes with redshift, then the haloes hosting the  $2 < z < 3$  sample will likely host the richest clusters of galaxies at  $z=0$ , whereas the haloes hosting the  $1.5 < z < 2.0$  sample will likely host poor to rich clusters at  $z=0$ . We conclude that ULIRGs at  $z \gtrsim 1$  signpost stellar buildup in galaxies that will reside in clusters at  $z = 0$ , with ULIRGs at increasing redshifts signposting the buildup of stars in galaxies that will reside in increasingly rich clusters.

*Subject headings:* galaxies: active — galaxies: starburst

## 1. Introduction

Among the core principles of current theories for the formation of large-scale structure is the premise that the evolution of the total mass distribution can be described by the evolution of Gaussian primordial density fluctuations, and that this evolution is traced by galaxies in some determinable way. Overdense ‘halos’ in the dark matter distribution are predicted to undergo successive mergers over time to build haloes of increasing mass, with galaxies forming from the baryonic matter in these haloes. This framework of ‘biased’ hierarchical buildup (Cole et al 2000; Granato et al 2000; Hatton et al 2003) has proven to be remarkably adept in explaining many aspects of galaxy and large-scale structure formation.

Comparing these predictions with observations is an active topic, and is particularly controversial concerning the evolution of massive galaxies (those with masses  $\gtrsim 10^{11} M_{\odot}$ ). The ‘naive’ expectation might be that massive galaxies form over a long period of time, as many halo mergers are needed to build up large baryon reservoirs, and indeed some massive galaxies do appear to form in this way (van Dokkum et al 1999; Tamura & Ohta 2003; Bell et al 2004). There is however observational evidence that many massive galaxies may form at high redshift and on short timescales (Dunlop et al 1996; Ellis et al 1997; Blakeslee et

al 2003), implying that the stars in massive local galaxies formed in less than a few Gyr of each other at  $z > 1$ . Further evidence has come from blank-field sub-mm surveys (Hughes et al 1998; Barger et al 1998; Eales et al 2000; Scott et al 2002; Borys et al 2003; Mortier et al. 2005), which have found a huge population of sub-mm bright sources (SMGs) at  $z \gtrsim 1$ , with IR luminosities of  $> 10^{12} L_\odot$ . SMGs are far more numerous than sources in the local Universe with comparable IR luminosities, the so-called Ultraluminous Infrared Galaxies (ULIRGs). These distant ULIRGs are good candidates for massive galaxies caught in the act of formation; they have a median redshift of  $z \simeq 2.5$  (Chapman et al 2005), high enough star formation rates to satisfy the observed color-scaling relationships in massive evolved systems, and a comparable comoving number density to local massive ellipticals. SMGs however pose a challenge for structure formation models, which invoke a diverse variety of solutions to explain the observed sub-mm counts (van Kampen et al 1999; Granato et al 2004; Baugh et al 2005; Bower et al 2006).

Progress on these issues requires observations that can be compared to models in a meaningful way, and one of the best ways is via measurement of clustering amplitudes. Massive haloes are predicted to cluster together on the sky, with the strength of clustering depending on their mass (Kaiser 1984; Bardeen et al 1986). If distant ULIRGs are the formation events of massive galaxies, then they should trace this clustering. Measuring clustering amplitudes for distant ULIRGs is however difficult; it requires a minimum of several hundred sources found over a significant area of sky (e.g. van Kampen et al 1999), but IR observatories available up to now cannot map large enough areas to the required depths to find this number of sources at  $z \gtrsim 1$ .

The launch of the Spitzer Space Telescope (Werner et al 2004) offers the potential to overcome these problems, due to its ability to map large areas of sky in the infrared to greater depths than any previous observatory. In this letter, we study the clustering of starburst-dominated ULIRGs in two redshift bins centered at  $z \sim 1.7$  and  $z \sim 2.5$ . We assume  $H_0 = 70 \text{ km s}^{-1} \text{ Mpc}^{-1}$ ,  $\Omega = 1$ , and  $\Omega_\Lambda = 0.7$ .

## 2. Analysis

To select high redshift, IR-luminous star-forming galaxies, we use the  $1.6\mu\text{m}$  emission feature, which arises due to photospheric emission from evolved stars. When this feature is redshifted into one of the IRAC channels then that channel exhibits a peak, or ‘bump’ compared to the other three channels (Simpson & Eisenhardt 1999; Sawicki 2002). A complete discussion of the source selection and characterization methods is given in Lonsdale et al 2006 (in preparation), which we summarize here.

Our sources are taken from three fields observed as part of the Spitzer Wide Area Infrared Extragalactic Survey (SWIRE, Lonsdale et al 2003); the ELAIS N1 and ELAIS N2 fields, and the Lockman Hole, covering 20.9 square degrees in total. We first selected those sources fainter than  $R=22$  (Vega), and brighter than  $400\mu\text{Jy}$  at  $24\mu\text{m}$ . Within this set, we selected two samples that displayed a ‘bump’ in the  $4.5\mu\text{m}$  and  $5.8\mu\text{m}$  channels, i.e. where  $f_{3.6} < f_{4.5} > f_{5.8} > f_{8.0}$  for one sample (the ‘B2’ sample) and where  $f_{3.6} < f_{4.5} < f_{5.8} > f_{8.0}$  for the other sample (the ‘B3’ sample). This resulted in a total of 1689 B2 sources and 1223 B3 sources.

For both samples we used the HYPER-Z code (Bolzonella et al 2000) to estimate redshifts, the results from which place most of the B2 sources within  $1.5 < z < 2.0$ , and most of the B3 sources within  $2.2 < z < 2.8$ . From the best fits we also derived IR luminosities and power sources, both of which are uncertain due to the photometric nature of the redshifts. The requirement that the sources have  $f_{24} > 400\mu\text{Jy}$  however demands an IR luminosity of  $\gtrsim 10^{12}\text{L}_\odot$  for all the sources. In most cases the SED fits predict that the dominant power source is a starburst, with star formation rates of  $\gtrsim 200\text{M}_\odot\text{yr}^{-1}$  (assuming a standard Salpeter IMF). Similarly, the presence of the  $1.6\mu\text{m}$  feature demands (accounting for uncertainties in redshift and stellar models) a minimum mass of evolved stars of  $\sim 10^{11}\text{M}_\odot$ . Both the B2 and B3 sources are thus good candidates for being moderately massive galaxies harboring an intense, obscured starburst, making them similar in nature to both local ULIRGs, and high-redshift SMGs.

We measure the angular clustering of both samples using the standard parametrization for the probability,  $p$ , of finding a source in a solid angle  $\Omega_1$ , and another object in another solid angle  $\Omega_2$  separated by an angle  $\theta$ :

$$p(\theta) = N^2[1 + \omega(\theta)]\Omega_1\Omega_2, \quad (1)$$

where  $N$  is the mean surface density of objects and  $\omega(\theta)$  is the angular two-point correlation function. We compute  $\omega(\theta)$  using the Landy & Szalay (1993) prescription, and divide  $\omega(\theta)$  by the “integral constraint” (Infante 1997) to correct for the finite size of the sample (though in both cases this correction was negligible). The survey area geometries are accounted for in the analysis by constructing coverage masks of the joint MIPS  $24\mu\text{m}$  and IRAC observations, and only considering those sources that lie within these masks.

We found that the levels of angular clustering seen in the three fields were consistent with each other to within  $0.5\sigma$ , with all three fields showing positive clustering for both the B2 and B3 samples. We therefore combined the angular clustering measures for each sample over the three fields. In Figure 1 we present the combined  $\omega(\theta)$  (with Poisson errors) vs.  $\theta$

plots for both samples. Both samples show a statistically significant detection of positive clustering on length scales of  $< 0.1^\circ$ . To quantify the strength of clustering, we fit both datasets with a single power law:

$$\omega(\theta) = A_\omega \theta^{1-\gamma} \quad (2)$$

where  $A_\omega$  is the clustering amplitude. A wide variety of sources are well fitted with  $\gamma = 1.8$  on small length scales (Bahcall et al 1983; Overzier et al 2003; Wilson 2003). We first check that our two datasets can be fit this way by allowing  $\gamma$  to vary and find that  $\gamma = 1.8$  is within  $1\sigma$  of the best-fit values. We therefore fix  $\gamma = 1.8$  and fit to get  $A_\omega = 0.0125 \pm 0.0017$  for the B3s and  $A_\omega = 0.0046 \pm 0.0011$  for the B2s.

### 3. Discussion

If a sample of galaxies with a measured  $\omega(\theta)$  also have a constrained redshift distribution, then we can derive the spatial correlation length,  $r_0(z)$ , of the sample by inverting Limber's equation (Limber 1953). For a redshift range spanning  $a$  to  $b$ , this can be expressed as:

$$\frac{r_0(z)}{f(z)} = \left[ \frac{H_0^{-1} A_\omega c C \left[ \int_a^b \frac{dN}{dz} dz \right]^2}{\int_a^b \left( \frac{dN}{dz} \right)^2 E(z) D_\theta^{1-\gamma}(z) f(z) (1+z) dz} \right]^{\frac{1}{\gamma}} \quad (3)$$

where  $f(z)$  parametrizes the redshift evolution of  $r_0$ ,  $D_\theta(z)$  is the angular diameter distance,  $c$  is the speed of light,  $dN/dz$  is the sample redshift distribution, and:

$$C = \frac{\Gamma(\gamma/2)}{\Gamma(1/2)\Gamma([\gamma-1]/2)}, E(z) = [\Omega_m(1+z)^3 + \Omega_\Lambda]^{\frac{1}{2}} \quad (4)$$

To compute  $r_0$  from Equation 3 requires a redshift distribution,  $dN/dz$ , but we have no spectroscopic redshifts for our sample. Therefore, we use analytic forms for  $dN/dz$  derived from the photometric redshift distributions (Lonsdale et al 2006). For the B2 sources this is a Gaussian centered at  $z = 1.7$  with a FWHM of 1.0, and for the B3 sources this is a Gaussian centered at  $z = 2.5$  with a FWHM of 1.2. The resulting correlation lengths are  $r_0 = 9.4 \pm 2.24 h^{-1} \text{Mpc}$  for the B2 sources, and  $r_0 = 14.4 \pm 1.99 h^{-1} \text{Mpc}$  for the B3 sources. As a check, we derived both redshift distributions using an independent code (Rowan-Robinson et al 2005), and found that the mean redshifts were the same, but that the FWHMs were

in both cases slightly broader. Although, in general, broader redshift distributions result in larger clustering amplitudes, in our case the effects are insignificant; for example if we use the Rowan-Robinson et al (2005) redshift distribution for the B3 sources then we obtain  $r_0 = 16.5 \pm 2.30 h^{-1} \text{Mpc}$ . To be conservative, we use the Lonsdale et al 2006 redshift distributions.

To place these clustering results in context, we consider two classes of model. The first parametrizes the spatial correlation function,  $\xi$ , as a single power law in comoving coordinates:

$$\xi(r_c, z) = \left(\frac{r_c}{r_0}\right)^{-\gamma} (1+z)^{\gamma-(3+\epsilon)} \quad (5)$$

where  $r_c$  is the comoving distance, and  $r_0$  is the comoving correlation length at  $z = 0$ . The comoving correlation length at a redshift  $z$ ,  $r_0(z)$ , can therefore be expressed as:

$$r_0(z) = r_0 f(z), f(z) = (1+z)^{\gamma-(3+\epsilon)} \quad (6)$$

where the choice of  $\epsilon$  determines the redshift evolution (Phillipps et al. 1978; Overzier et al 2003). Generally, models that use this parametrization are those where the correlation length increases or remains constant with decreasing redshift; these can be thought of as tracing the clustering evolution of a given halo. Several cases are usually quoted. First is ‘comoving clustering’, where haloes expand with the Universe, and  $\epsilon = \gamma - 3$ ; in this case clustering remains constant with redshift. Second is the family of models for which  $\epsilon \geq 0$ , for which clustering increases with time. Examples of this family include (a) ‘stable’ clustering, for which  $\epsilon \simeq 0$  (in this case the size of the haloes is frozen in proper coordinates, hence comoving expansion of the background mass distribution makes the halo clustering grow stronger), (b) the predicted evolution of clustering of the overall dark matter distribution, where  $\epsilon \simeq \gamma - 1$  (Carlberg et al 2000), and  $r_0 \simeq 5$  at  $z=0$  (Jenkins et al 1998), (c) ‘linear’ clustering, where  $\epsilon = 1.0$ . A cautionary note to this is that detailed interpretations of clustering evolution from these models suffer from several theoretical flaws (Moscardini et al 1998; Smith et al. 2003), and so should be thought of as qualitative indicators rather than quantitative predictions. We therefore simply use the ‘stable’ and ‘linear’ models as indicators of the possible range of halo clustering amplitude with redshift.

The second class of model comprises those in which comoving correlation lengths increase with *increasing* redshift. These models introduce ‘bias’,  $b(z)$ , between the galaxies and the underlying dark matter. An example of such models are the ‘fixed mass’ models (Matarrese et al 1997; Moscardini et al 1998), which assume that galaxies selected in a certain way

predominantly occupy haloes of the same mass. These models therefore predict the clustering strength of haloes of a specified mass at any given redshift. In Figure 2 we plot the  $\epsilon$  model for dark matter, ‘stable’ and ‘linear’ epsilon models normalized to the B2 and B3 clustering strengths, the fixed halo mass models for halo masses of  $10^{12}M_{\odot}$ ,  $10^{13}M_{\odot}$ , and  $10^{14}M_{\odot}$ , the  $r_0$  values for the B2 and B3 galaxies, and the spatial correlation lengths of other galaxy populations taken from the literature.

Considering these uncertainties, care must be taken when comparing the models to observed galaxy correlation lengths. With this in mind, we use Figure 2 to explore the relationships between our samples, the underlying dark matter, and other galaxies. Considering first other measured or predicted correlation lengths at the same redshift, then both samples are very strongly clustered, with correlation lengths much higher than that predicted for the overall DM distribution at their respective epochs. Both B2s and B3s cluster significantly more strongly than optical QSOs at their respective epochs, and B3s cluster more strongly than sub-mm selected galaxies. Based on the Matarrese et al (1997) models, then we derive *approximate*  $1\sigma$  halo mass ranges of  $10^{13.7} < M_{\odot} < 10^{14.1}$  for the B3s, and  $10^{13.5} < M_{\odot} < 10^{13.9}$  for the B2s.

The most interesting comparison is however between the two samples themselves. The clustering evolution of QSOs with redshift (Croom et al. 2005) may mean that there is a ‘minimum’ host halo mass for QSO activity, below which no QSO is seen, of  $\sim 5 \times 10^{12}M_{\odot}$ . The correlation lengths for the B2 and B3 samples are consistent with the same conclusion but for a higher halo mass, tracing the clustering line for a  $\sim 6 \times 10^{13}M_{\odot}$  DM halo. Interestingly, from Figure 2 we would draw a similar conclusions for optically faint LBGs, albeit for a halo mass of  $\sim 10^{12}M_{\odot}$  (see also Adelberger et al. (2005)). Taken together, these results imply that a minimum halo mass is an important threshold factor for *all* forms of very luminous activity in galaxies, both starbursts and AGN. It is also interesting to speculate on what the host haloes of B2 and B3 sources contain at lower and higher redshifts. We might expect that a halo hosting a B3 source could contain an optically bright LBG at  $z \sim 4$  when its mass is  $\sim 10^{13.2}M_{\odot}$ , followed by a B3 at  $z \sim 2.5$  once the halo has reached  $\sim 10^{14}M_{\odot}$ , possibly accompanied by other (near-IR selected) star forming systems (Daddi et al. 2004, 2005), before evolving to host an extremely rich galaxy cluster at low redshifts, with a halo mass substantially exceeding  $10^{15}M_{\odot}$ . The occupants of a halo hosting a B2 galaxy would however probably be different. We would expect that such a halo could contain an SMG at  $z \sim 2.5$ , and optically fainter LBGs at  $4 < z < 5$  (though probably not LBGs at  $z \sim 3$ ). At lower redshifts such a halo might host a radio-bright AGN and or ERO at  $z \sim 1$ , and a (poor to rich) cluster at  $z = 0$ . These evolutionary paths for the B2s and B3s are consistent with semi-analytic models and numerical simulations (Governato et al. 1998; Nagamine 2002) which predict that LBGs at high redshift evolve into local clusters.

We conclude that ULIRGs at  $z \gtrsim 1.5$  as a class likely signpost stellar buildup in galaxies in clusters at  $z = 0$ , with higher redshift ULIRGs signposting stellar buildup in galaxies that will reside in more massive clusters at lower redshifts. These predictions are however sensitive to the assumed form of DM halo growth, and should be regarded with caution.

We thank Emanuele Daddi for saving our lives, Andy Connolly for useful discussion, and the referee for a very helpful report. SJO acknowledges a Leverhulme Fellowship. Support for this work, part of the Spitzer Space Telescope Legacy Science Program, was provided by NASA through an award issued by JPL under NASA contract 1407. This research was carried out, in part, by JPL, California Institute of Technology, and was sponsored by NASA.

## REFERENCES

Adelberger, K. L., Steidel, C. C., Pettini, M., Shapley, A. E., Reddy, N. A., & Erb, D. K. 2005, ApJ, 619, 697

Allen, P. D., Moustakas, L. A., Dalton, G., MacDonald, E., Blake, C., Clewley, L., Heymans, C., & Wegner, G. 2005, MNRAS, 360, 1244

Bahcall N. A., Soneira R. M., 1983, ApJ, 270, 20

Bardeen, J. M., Bond, J. R., Kaiser, N., & Szalay, A. S. 1986, ApJ, 304, 15

Barger A. J., Cowie L. L., Sanders D. B., Fulton E., Taniguchi Y., Sato Y., Kawara K., Okuda H., 1998, Nat, 394, 248

Baugh, C. M., Lacey, C. G., Frenk, C. S., Granato, G. L., Silva, L., Bressan, A., Benson, A. J., & Cole, S. 2005, MNRAS, 356, 1191

Bell, E. F., et al 2004, ApJ, 608, 752

Blain A. W., Chapman S. C., Smail I., Ivison R., 2004, ApJ, 611, 725

Blakeslee, J. P., et al 2003, ApJ, 596, L143

Bolzonella M., Miralles J.-M., Pello R., 2000, A&A, 363, 476

Borys, C., Chapman, S., Halpern, M., & Scott, D. 2003, MNRAS, 344, 385

Bower R., G., et al 2006, MNRAS, submitted, astroph 0511338

Carlberg, R. G., Yee, H. K. C., Morris, S. L., Lin, H., Hall, P. B., Patton, D., Sawicki, M., & Shepherd, C. W. 2000b, *ApJ*, 542, 57

Carroll, S. M., Press, W. H., & Turner, E. L. 1992, *ARA&A*, 30, 499

Chapman S. C., Blain A. W., Smail I., Ivison R. J., 2005, *ApJ*, 622, 772

Cole, S., Lacey, C. G., Baugh, C. M., & Frenk, C. S. 2000, *MNRAS*, 319, 168

Croom S. M., et al. 2005, *MNRAS*, 356, 415

Daddi, E., et al. 2004, *ApJ*, 600, L127

Daddi, E., et al. 2005, *ApJ*, 631, L13

Dunlop J., Peacock J., Spinrad H., Dey A., Jimenez R., Stern D., Windhorst R., 1996, *Nat*, 381, 581

Eales S., Lilly S., Webb T., Dunne L., Gear W., Clements D., Yun M., 2000, *AJ*, 120, 2244

Ellis R. S., Smail I., Dressler A., Couch W. J., Oemler A., Butcher H., Sharples R. M., 1997, *ApJ*, 483, 582

Georgakakis, A., Afonso, J., Hopkins, A. M., Sullivan, M., Mobasher, B., & Cram, L. E. 2005, *ApJ*, 620, 584

Governato, F., Baugh, C. M., Frenk, C. S., Cole, S., Lacey, C. G., Quinn, T., & Stadel, J. 1998, *Nature*, 392, 359

Granato, G. L., Lacey, C. G., Silva, L., Bressan, A., Baugh, C. M., Cole, S., & Frenk, C. S. 2000, *ApJ*, 542, 710

Granato, G. L., De Zotti, G., Silva, L., Bressan, A., & Danese, L. 2004, *ApJ*, 600, 580

Hatton, S., Devriendt, J. E. G., Ninin, S., Bouchet, F. R., Guiderdoni, B., & Vibert, D. 2003, *MNRAS*, 343, 75

Hughes D. H., et al, 1998, *Nat*, 394, 241

Infante L., 1997, *A&A*, 282, 353

Jenkins A., et al, 1998, *ApJ*, 499, 20

Kaiser, N. 1984, *ApJ*, 284, L9

Landy S. D. & Szalay A. S., 1993, *ApJ*, 412, 64

Limber, D. N. 1953, *ApJ*, 117, 134

Lonsdale C. J., et al, 2003, *PASP*, 115, 897

Lonsdale, C., et al 2006, *ApJ*, in preparation

Matarrese, S., Coles, P., Lucchin, F., & Moscardini, L. 1997, *MNRAS*, 286, 115

Mortier, A. M. J., et al. 2005, *MNRAS*, 363, 563

Moscardini, L., Coles, P., Lucchin, F., & Matarrese, S. 1998, *MNRAS*, 299, 95

Nagamine, K. 2002, *ApJ*, 564, 73

Ouchi, M., et al. 2004, *ApJ*, 611, 685

Overzier R. A., Rottgering H. J. A., Rengelink R. B., Wilman R. J., 2003, *A&A*, 405, 53O

Phillipps, S., Fong, R., Fall, R. S., & MacGillivray, H. T. 1978, *MNRAS*, 182, 673

Rowan-Robinson M., et al, 2005, *AJ*, 129, 1183

Sawicki, M. 2002, *AJ*, 124, 3050

Scott S. E., et al, 2002, *MNRAS*, 331, 817

Simpson, C., & Eisenhardt, P. 1999, *PASP*, 111, 691

Smith, R. E., et al. 2003, *MNRAS*, 341, 1311

Tamura, N., & Ohta, K. 2003, *AJ*, 126, 596

van Dokkum, P. G., Franx, M., Fabricant, D., Kelson, D. D., & Illingworth, G. D. 1999, *ApJ*, 520, L95

van Kampen, E., Jimenez, R., & Peacock, J. A. 1999, *MNRAS*, 310, 43

Werner M. W., et al, 2004, *ApJS*, 154, 1

Wilson, G. 2003, *ApJ*, 585, 191

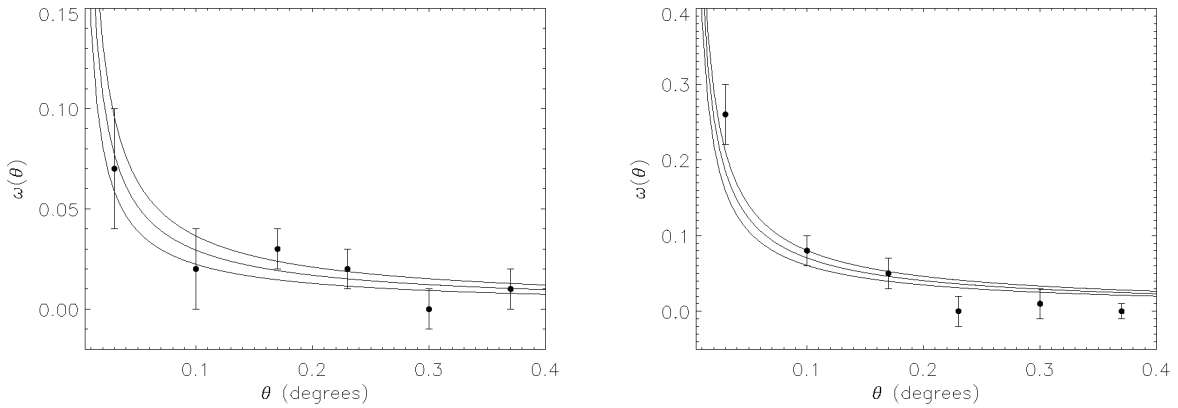


Fig. 1.— The two-point correlation function and (Poisson) error bars as a function of  $\theta$  for (left) the B2 sample, and (right) the B3 sample, in 4' bins. The three lines show the best-fit power law, and the 1 $\sigma$  limits.

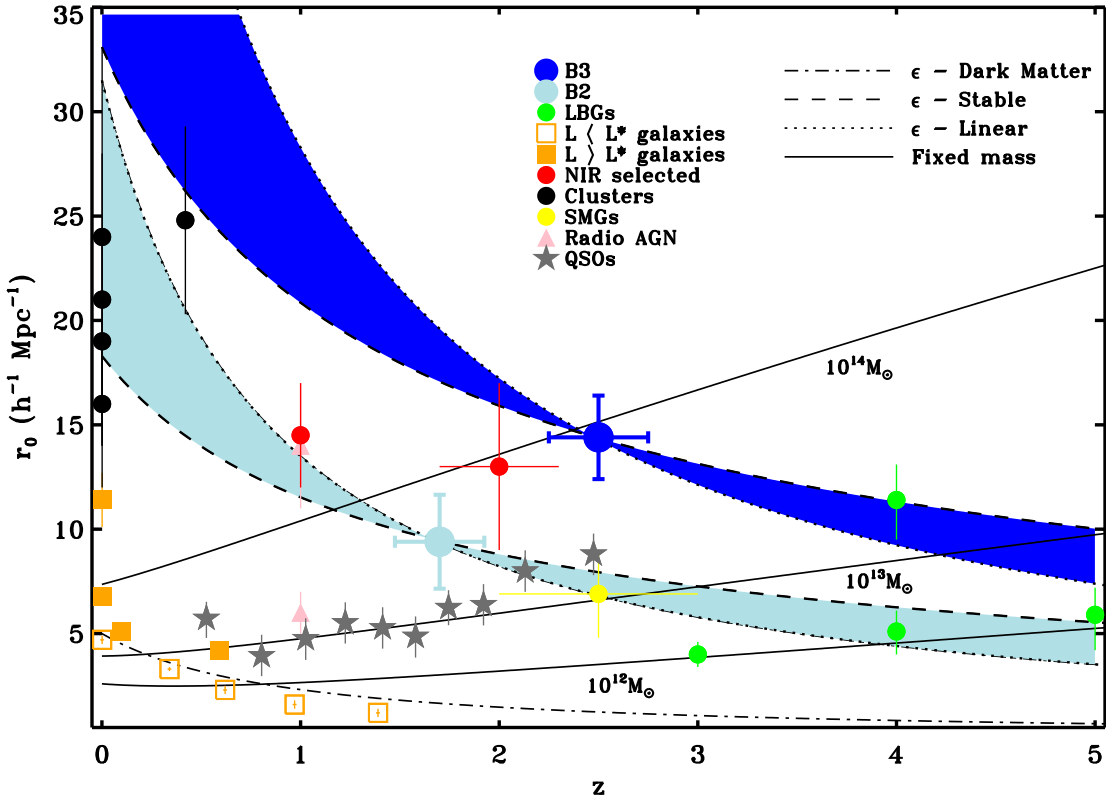


Fig. 2.— Comoving correlation length,  $r_0$ , vs. redshift. Other data are taken from Moscardini et al 1998; Overzier et al 2003; Daddi et al. 2004; Blain et al 2004; Ouchi et al. 2004; Adelberger et al. 2005; Croom et al. 2005; Georgakakis et al. 2005; Allen et al. 2005. The ‘Fixed mass’ lines show the predicted clustering amplitude of haloes of a given mass at any particular redshift, whereas the  $\epsilon$  lines show the predicted clustering amplitude of an individual halo for three halo growth models, described in the text. The ‘Stable’ and ‘Linear’ lines give a qualitative indicator of the range of how DM haloes may grow with redshift, and we have normalized ‘Stable’ and ‘Linear’ lines to the clustering amplitudes of the B2s and the B3s. The shaded regions therefore indicate what these haloes may host at lower and higher redshifts. - the haloes hosting B3s may contain an optically bright LBG at  $z \simeq 4$  (upper green point), and grow to host very rich galaxy clusters at  $z=0$ , whereas the haloes hosting B2 sources may contain optically fainter LBGs at  $4 < z < 5$ , SMGs at  $z \sim 2.5$ , radio-bright AGN (upper pink triangle) and (old) EROs at  $z \simeq 1$ , and poor to rich clusters at  $z=0$ .